


Cite this: *RSC Adv.*, 2020, 10, 3184

# Comparative study of Ni(II) adsorption by pristine and oxidized multi-walled N-doped carbon nanotubes

Renata Balog,<sup>a</sup> Maryna Manilo,<sup>b</sup> \*<sup>b</sup> Laszlo Vanyorek,<sup>c</sup> Zoltan Csoma<sup>a</sup> and Sandor Barany<sup>a,c,d</sup>

The principles and mechanisms of adsorption of Ni(II) ions by well characterized pristine and oxidized N-doped multi-walled carbon nanotubes (N-CNTs) are described and discussed. The samples were synthesized by CCVD method using *n*-butylamine as the carbon source and Ni(NO<sub>3</sub>)<sub>2</sub> + MgO as the catalyst and purified by treatment with HCl. The surface functionalization was performed using oxidation with a mixture of concentrated H<sub>2</sub>SO<sub>4</sub> and HNO<sub>3</sub>. The morphology, nature and charge of surface groups were characterized by HRTEM, XPS, FTIR and micro-electrophoresis methods. It has been shown that: adsorption of Ni(II) reaches an equilibrium value within 20–30 min; the degree of extraction of nickel ions from the solution increases with its dilution; adsorption of Ni(II) results in an insufficient decrease in the suspension pH for pristine N-CNTs (0.5–0.6 pH unit) and considerable lowering of the pH for the oxidized sample (up to 2.5 pH unit); the adsorption isotherms are described by the Langmuir equation; the plateau amounts of adsorption (35–40 mg g<sup>−1</sup>) are almost the same for both as-prepared and oxidized samples; at pH 8 and higher a sharp increase in adsorption is observed which is caused by nickel hydroxide precipitation. The spectroscopic, adsorption, electrophoretic and pH measurement data testify that below pH 8 the major mechanism of adsorption by as-prepared N-CNTs is the donor–acceptor interaction between the free electron pair of N atoms incorporated into the nanotube lattice and vacant d-orbital of the adsorbing Ni(II) ions. For the oxidized N-CNTs ion-exchange processes with a release of H<sup>+</sup> play a decisive role.

Received 21st November 2019

Accepted 11th January 2020

DOI: 10.1039/c9ra09755d

rsc.li/rsc-advances

## Introduction

Among the variety of practical applications of carbon nanotubes (CNTs) an increasingly important segment is related to their use as sorbents for toxic substances, heavy metal ions, and organic compounds.<sup>1</sup> For example, CNTs are intensely studied as sorbents for water purification from individual lead,<sup>2</sup> nickel, copper, cobalt,<sup>3</sup> and chromium<sup>4</sup> ions, and other individual or mixed ions of different metals.<sup>5</sup>

Nickel(II) is one of most hazardous heavy metal ions which is increasingly accumulated in potable, ground and wastewaters. There are numerous studies devoted to extraction of Ni(II) by single-walled (SWCNTs) or multi-walled carbon nanotubes (MWCNTs), both pristine and oxidized by different oxidizing agents. The kinetics of adsorption, shape of adsorption isotherms, and impact of pH, foreign ions and degree of CNT

surface functionalization has been elucidated. A short review of the recent results obtained is summarized below.

Authors<sup>6,7</sup> have shown that the adsorption of Ni(II) onto oxidized CNTs is strongly dependent on pH and nanotube concentration and, to a lesser extent, ionic strength. The adsorption data fit the Langmuir model well, and the adsorbed Ni(II) can be easily desorbed at pH < 2.0. It was speculated that ion exchange might be the predominant mechanism of Ni(II) adsorption on oxidized CNTs. Adsorption of Ni(II) on oxidized CNTs increased from zero to 99% at pH 2–9, and then maintained the high level with increasing pH. The adsorption achieved equilibrium within 2 h.<sup>7</sup> The mechanism of adsorption was attributed to surface complexation and ion exchange. Also it was shown that the adsorption capacity for nickel ions from aqueous solutions increased significantly onto the surface of the oxidized CNTs compared to that on the as-produced CNTs, and the maximum adsorption by these adsorbents was determined as 18.08 mg g<sup>−1</sup> and 49.26 mg g<sup>−1</sup>, respectively.<sup>8</sup> The number of functional groups, total acidic sites and negatively charged carbons on CNTs surface were greatly increased after oxidation by NaOCl, which resulted in sorption of more nickel ions.<sup>9</sup> Typically, 60–95% of Ni(II) can be extracted from aqueous solution by MWCNTs depending on the initial solution concentrations. As it

<sup>a</sup>The Transcarpathian II Ferenc Rakoczi Hungarian Institute, Kossuth sq. 6, Beregovo, Ukraine

<sup>b</sup>F. D. Ovcharenko Institute of Biocolloidal Chemistry, National Academy of Sciences of Ukraine, Vernadskyi blvd. 42, Kyiv, Ukraine. E-mail: assoL\_M@i.ua

<sup>c</sup>Institute of Chemistry, University of Miskolc, 3515 Miskolc-Egyetemvaros, Hungary

<sup>d</sup>MTA-ME Materials Science Research Group, 3515 Miskolc-Egyetemvaros, Hungary


is suggested by the distribution coefficient values, increased initial Ni(II) solution concentrations resulted in lower adsorption, while the total amount of ions removed from the equilibrating solutions increased. Higher adsorption was observed at pH > 6.0, and the sorption process reached equilibrium at 60 min. The sorption mechanisms are complicated and appear attributable to electrostatic forces and chemical interactions between the nickel ions and the surface functional groups of the CNTs.<sup>10</sup>

Rao *et al.* (2007)<sup>11</sup> reviewed the laws and mechanisms of sorption of divalent metal ions ( $\text{Cd}^{2+}$ ,  $\text{Cu}^{2+}$ ,  $\text{Ni}^{2+}$ ,  $\text{Pb}^{2+}$ , and  $\text{Zn}^{2+}$ ) from aqueous solution by various kinds of raw and surface oxidized CNTs. Chemical interactions between the metal ions and surface functional groups were considered to be the main adsorption mechanism. The sorption capacities of CNTs remarkably increased after oxidized by NaOCl,  $\text{HNO}_3$  and  $\text{KMnO}_4$  solutions and reached, for example, 6.9 mg Ni  $\text{g}^{-1}$  and 47.8 mg Ni  $\text{g}^{-1}$  onto CNTs oxidized by  $\text{HNO}_3$  or NaOCl, respectively. Authors<sup>12</sup> have analysed in detail the impact of CNTs properties (adsorption sites, pore volume, BET surface area, surface total acidity) and solution properties (ionic strength, effect of pH) on the adsorption of heavy metal ions by carbon nanotubes. The contribution of physical adsorption, electrostatic attraction, precipitation and chemical interaction between the metal ions and the surface functional groups of CNTs was discussed.

Multi-walled carbon nanotube/iron oxide magnetic composites turned out to be efficient adsorbents and solidifications of Ni(II) and Sr(II) ions.<sup>13</sup> The adsorption of these ions on the magnetic composites was shown to be strongly dependent on pH and ionic strength. The adsorption capacity of the magnetic composites was much higher than that of MWCNTs and iron oxides individually. Results of desorption study showed that Ni(II) adsorbed onto the magnetic composites can be easily desorbed at pH < 2.0.

Authors<sup>14</sup> measured the adsorption isotherms of Cu(II), Ni(II), Zn(II) and Cd(II) onto CNTs oxidized by concentrated  $\text{HNO}_3$  in single, binary, ternary and quaternary systems and have shown that isotherms reveal the effect of competition for adsorption sites seen as a decrease in the amount adsorbed. The uptakes at the equilibrium concentration of 0–0.04 mmol  $\text{dm}^{-3}$  in single system and 0–0.15 mmol  $\text{dm}^{-3}$  in binary system are in the order  $\text{Cu}^{2+} > \text{Ni}^{2+} > \text{Cd}^{2+} > \text{Zn}^{2+}$  while for the ternary and quaternary, the order is  $\text{Cu}^{2+} > \text{Cd}^{2+} > \text{Zn}^{2+} > \text{Ni}^{2+}$ .

Summarizing the literature review we can say that the major factors affecting the adsorption of Ni(II) by carbon nanotubes and the mechanisms of the process are at large clarified. At the same time, surprisingly, there is a lack of information about the laws and mechanisms of adsorption of Ni(II) by N-doped carbon nanotubes, *i.e.* adsorbents containing surface N atoms in different state, potentially capable to form complexes with Ni(II) ions. We tried to fill in, at least in part, this gap.

## Experimental

### Materials

**Synthesis and functionalization of N-CNTs.** The N-doped carbon nanotubes (N-CNTs) were synthesized by Catalytic

Chemical Vapour Deposition (CCVD) method using *n*-butylamine (VWR) as carbon source and  $\text{Ni}(\text{NO}_3)_2 \cdot 6\text{H}_2\text{O}$  (Sigma Aldrich) plus magnesium oxide, MgO (Merck) as catalyst materials, as described in the paper.<sup>15</sup> The product was purified from the catalyst by treatment with concentrated hydrochloride acid (VWR). The surface functionalization of N-CNTs was performed using oxidation with mixture of concentrated sulphuric and nitric acids ( $v/v = 3 : 1$ ) at 80 °C overnight using continuous stirring. After the acidic treatment the N-CNTs were filtered and washed with distilled water until pH 5–6 was reached, and then dried at 120 °C. The mixture of  $\text{H}_2\text{SO}_4$  and  $\text{HNO}_3$  turned out to be very efficient for oxidation of CNTs as it was shown in our previous work.<sup>16</sup> The presence of the –OH and –COOH functional groups on the surface was confirmed by X-ray Photoelectron Spectroscopy (XPS) and Fourier-transfer infrared spectroscopy (FTIR) measurements. The BET surface of the untreated N-CNT was 131  $\text{m}^2 \text{g}^{-1}$  which was increased to 146  $\text{m}^2 \text{g}^{-1}$  after oxidation.

### Methods

**Spectroscopy.** A VERTEX 70 FTIR spectrometer (Bruker, Germany) was used to record the spectra of the samples at wavelengths  $\lambda = 4000\text{--}400 \text{ cm}^{-1}$  and a resolution of  $\approx 4 \text{ cm}^{-1}$ . Before the measurements, the samples were exposed for 24 h at 25 °C and mixed with spectroscopic dry potassium bromide. The mixture containing 0.03 wt% (here and after %) CNTs was thoroughly attired in an agate mortar, and a pellet to be used for the measurements was prepared using a hydraulic press.

**Electrophoresis.** The electrophoretic mobility of CNTs in aqueous media was determined using the ZetaSizer Nano ZS instrument (Malvern, United Kingdom). Before the measurements, 0.01% CNT dispersion was treated in an ultrasonic bath (Tesla, Czech Republic) at a frequency of 35 kHz for 30 min. A sample was taken with a pipette from the upper part of the dispersion for the measurements which were performed at room temperature ( $T = 298 \text{ K}$ ) in the range of external electric field gradients of 6–15  $\text{V cm}^{-1}$ . The electrophoretic mobility was transformed into  $\zeta$ -potential using the classical Smoluchowski equation approach with the software of the instrument. This approach does not take into account the breaking effect of induced dipole moments on electrophoresis that arises in the event of electric double layer (EDL) polarization that is possible for thick double layers, *i.e.* at low ionic strength values. Therefore, the given below values of the electrokinetic potential represent some “efficient”  $\zeta$ -potentials equal to the electrophoretic mobility multiplied by the ratio of the viscosity of the medium to its permittivity. Such a procedure is widely accepted in the literature, and it can serve for comparison purposes, *i.e.* to follow the effect of different variables on the electrophoretic mobility and  $\zeta$ -potential. The presented values of the  $\zeta$ -potential were obtained by averaging three to six measurement results; the measurements error was about 3%.

**Morphology.** The morphology of the N-CNTs was studied by High Resolution Transmission Electron microscopy, HRTEM (FeiTechnai G2, 200 kV). The samples for measurements were prepared by dropping aqueous dispersion onto carbon layered



copper grids (Carbon/Copper grids, 300 Mesh, Ted Pella Inc.). The XPS (SPECS instrument with PHOIBUS 150 MCD 19 detector) was used to identify the chemical bounds of the incorporated nitrogen atoms and surface functional groups.

**Adsorption measurements.** Ni(II) ions were adsorbed by the carbon nanotubes (typical adsorbent concentration of 0.1%) at room temperature ( $T = 298\text{ K}$ ) in a pH range of 2.0–12.0 under mechanical shaking the reaction mixtures for designated period of time. The kinetic dependencies were measured during 360 h. The concentration of nickel ions before and after adsorption was determined in acetylene–air flame with an Agilent 240AA atomic absorption spectrophotometer (Agilent Technologies, US) operating at a wavelength of 429.0 nm and an optical gap width of 0.5 nm. The chosen conditions enable to determine the concentration of Ni(II) ions in the range of 1–100  $\mu\text{g dm}^{-3}$ . The adsorbed amount was calculated from the material balance of Ni(II) ions in solution before and after adsorption. The reproducibility of measurements was below 5%.

The changes of pH in the N-CNT suspensions containing NiCl<sub>2</sub> solution were determined in the following way. To 10 cm<sup>3</sup> of NiCl<sub>2</sub> solution of concentration 29.3 mg dm<sup>-3</sup> (5 mmol dm<sup>-3</sup>) with adjusted (by adding HCl or NaOH) pH values, 10 mg (9.9–10.1 mg) N-CNT was added. The suspension was shaking 30 minutes, then it was filtered, the equilibrium pH value was measured and the concentration of Ni(II) ions in the supernatant was determined as described above.

## Results and discussion

### Characterization of N-doped carbon nanotubes

**HRTEM study of non-oxidized and oxidized N-CNTs.** The HRTEM picture demonstrates that non-oxidized N-CNTs represent uneven fibers with length of 2–3  $\mu\text{m}$ , and diameter between 7 nm and 22 nm, with a mean value of 12.4 nm (Fig. 1a). As a result of oxidative treatment, the N-CNTs fibers were broken into shorter fibers, with about 200–800 nm sections in length (Fig. 1b). This can be attributed to the fact that the N-doped bamboo-like carbon nanotubes are easily ruptured, because their mechanical strength is lower compared to their non-doped counterparts. The extraordinary structure of these nanotubes is demonstrated on their schematic illustration (Fig. 1c). A number of graphene edges are seen on the wall of N-CNTs, containing sp<sup>3</sup> carbon atoms and nitrogen atoms, which easily react with oxidants (Fig. 1d). In this sense the N-CNTs can be oxidized to higher extent than the non-doped, conventional MWCNTs or SWCNTs. The fiber edges can serve as high energy adsorption sites on the wall of bamboo-like nanotubes which are easily accessible for different ions or molecules and can form relatively strong bounds with the adsorbent surface (due to ion exchange adsorption, surface complexes or  $\pi$ – $\pi$  interactions).

**Spectroscopic characterization.** XPS and FTIR measurements were applied to identify the binding types and the nature of surface functional groups. Fig. 2 shows the XPS spectra of non-oxidized and oxidized N-CNTs characterizing the binding energy of C–N and C–O bounds. The XPS spectrum of non-oxidized N-CNTs demonstrates the presence of specific

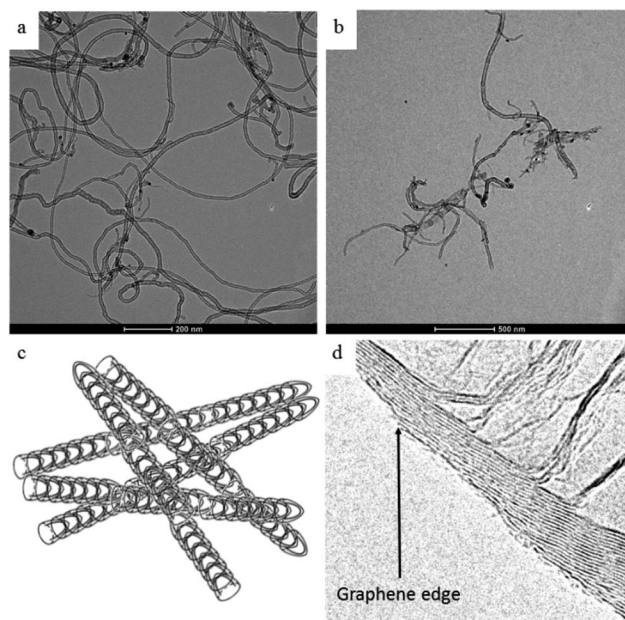


Fig. 1 HRTEM image of the non-oxidized (a) and the oxidized (b) N-CNTs. Schematic illustration of the bamboo like structure (c). The graphene edges on the nanotube wall (d).

chemical binding, which is typical for the N-doped CNTs (Fig. 2a). The peak at 398.6 eV binding energy can be attributed to the pyridine type nitrogen atoms (Fig. 2a), the next peak at 401.1 eV originates from the graphitic nitrogen incorporation. A peak of the oxidized nitrogen (pyridine N<sup>+</sup>–O<sup>–</sup> species) can be

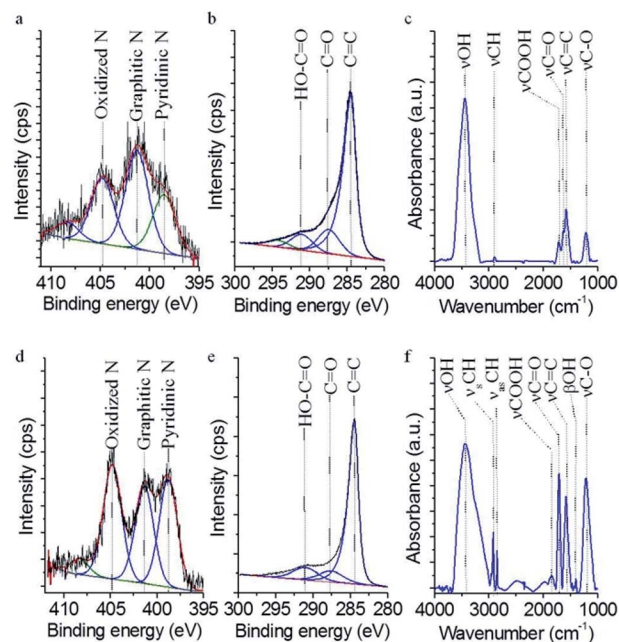


Fig. 2 XPS spectra with deconvoluted N 1s band of the non-oxidized (a) and oxidized (d) N-CNTs and C 1s band of non-oxidized (b) and oxidized (e) N-CNTs. FTIR spectrum of the non-oxidized (c) and oxidized (f) carbon nanotubes.





also observed on the spectrum, at 404.7 eV binding energy. The N-doped carbon nanotubes are easily oxidized at crystal distortions in the graphitic structure. During the acidic treatment, oxygen containing functional groups are developed, which are located at the C 1s band (Fig. 2b). The appearance of  $\text{C}=\text{C}$  and  $\text{C}-\text{C}$  bonds is reflected by a highly intensive peak at 284.6 eV, and the  $\text{C}=\text{O}$  peak was also identified at 287.5 eV (Fig. 2b). The peak of the carboxyl groups is shown at 291.2 eV binding energy. These oxygen-containing functional groups are visible on the FTIR spectra (Fig. 2c and f): stretching vibration of the  $\text{C}-\text{O}$  bond at  $1205\text{ cm}^{-1}$ , carbonyl bond at  $1628.7\text{ cm}^{-1}$ , carboxyl groups at  $1713.7\text{ cm}^{-1}$  and hydroxyl groups at  $3440.7\text{ cm}^{-1}$  (Fig. 2c). The latter bond is originated from the alcoholic or phenolic hydroxyl groups and from the  $-\text{COOH}$  groups. Adsorbed water can contribute to the appearance of this absorption band as well. The vibration mode of N-CNT structure ( $\nu\text{C}=\text{C}$ ) was also found in the FTIR spectrum at  $1565.4\text{ cm}^{-1}$  wavenumber (for a detailed information about FTIR spectra see, e.g. article<sup>17</sup>).

Visual presentation of the positions and states of the N-atom in the N-doped carbon nanotubes lattice, with corresponding binding energies, is given by Fig. 3. Theoretically all of them can participate in binding the  $\text{Ni(II)}$  ions to the CNT surface alongside with cation exchange with surface functional groups.

The interaction of  $\text{Ni(II)}$  ions with oxidized N-CNTs was examined by comparing the FTIR spectra of pure carbon nanotubes and those containing adsorbed nickel in amount that corresponds to saturation value. The peaks which are typical for the oxidized N-CNTs are shown on Fig. 4. For "pure" N-CNTs, bands of the surface hydroxyl groups are located at  $3426\text{ cm}^{-1}$  ( $\nu\text{OH}$ ) and  $1396\text{ cm}^{-1}$  ( $\beta\text{OH}$ ) while the  $\text{C}-\text{O}$  stretching ( $\nu\text{C}-\text{O}$ ) vibration mode at  $1175\text{ cm}^{-1}$  wave number. In the event of nickel-containing samples the peaks were shifted, and the band positions were found at  $3306\text{ cm}^{-1}$  ( $\nu\text{OH}$ ),  $1380\text{ cm}^{-1}$  ( $\beta\text{OH}$ ) and  $1191\text{ cm}^{-1}$  ( $\nu\text{C}-\text{O}$ ), correspondingly. These regularities can be explained by interactions between the  $\text{Ni(II)}$  ions and

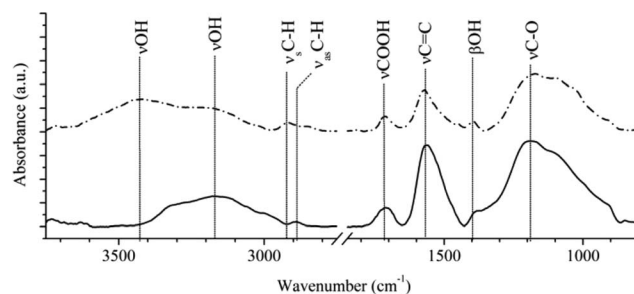


Fig. 4 FTIR spectra of the oxidized N-CNTs before (upper line) and after (lower line) nickel adsorption.

nanotubes surface functional groups. Also it was found that  $\text{C}=\text{C}$  stretching vibration ( $\nu\text{C}=\text{C}$ ) band was shifted from  $1571\text{ cm}^{-1}$  to  $1560\text{ cm}^{-1}$  as a result of adsorption of nickel ions. This is an evidence of interaction of between the  $\text{Ni(II)}$  ions and delocalized electron cloud of carbon nanotubes. Minimal shift can also be seen for the carboxylic ( $\nu\text{COOH}$ ) band.

### Electrokinetic potential

Fig. 5 shows the pH-dependence of N-CNTs electrokinetic potential in aqueous suspension. For the pristine N-CNT samples, the isoelectric point (IEP) is observed near pH 7.2, which is higher than the IEP values reported for regular (no N atoms in the lattice) MWCNTs: pH 4.0 (ref. 18) or pH 6.0.<sup>19</sup> This means that at lower pH, the surface is charged positively. The positive charge of the surface in acidic media (pH 3–7) is due to the presence of small amounts of oxidized species in the original N-CNTs (see spectra on Fig. 2) as well as to the presence of pyridine type N atoms in the lattice capable to acquire positive charge due to proton transfer. The shift of the IEP to higher values probably reflects the contribution of protonated N-atoms into the CNT surface charge. After the acid treatment the isoelectric point is not reached, and the surface charge remains negative in the whole pH interval studied (pH 3.0–11.8). This is

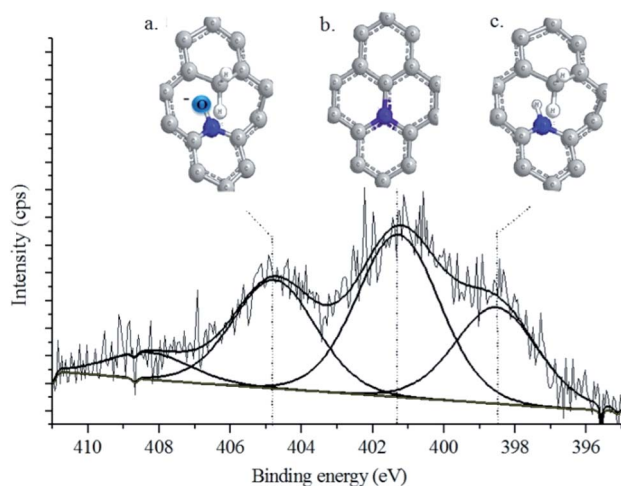


Fig. 3 XPS spectra of N-doped carbon nanotubes with schematic illustration of positions/states of the N atom in the CNT lattice, with corresponding binding energy.

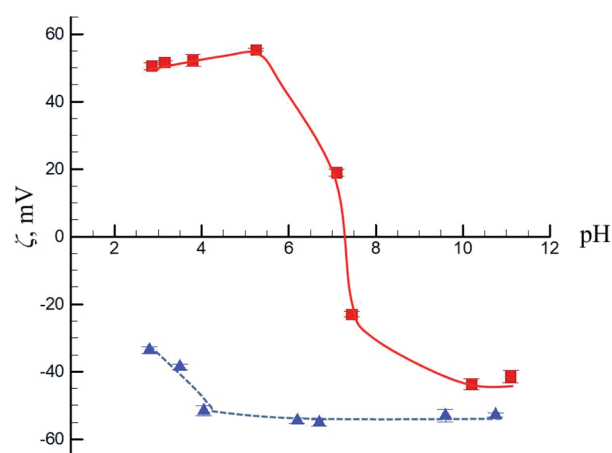


Fig. 5 Dependence of the  $\zeta$ -potential of pristine (squares) and oxidized (triangles) N-CNTs on the system pH. Concentration of N-CNTs was 0.1%.



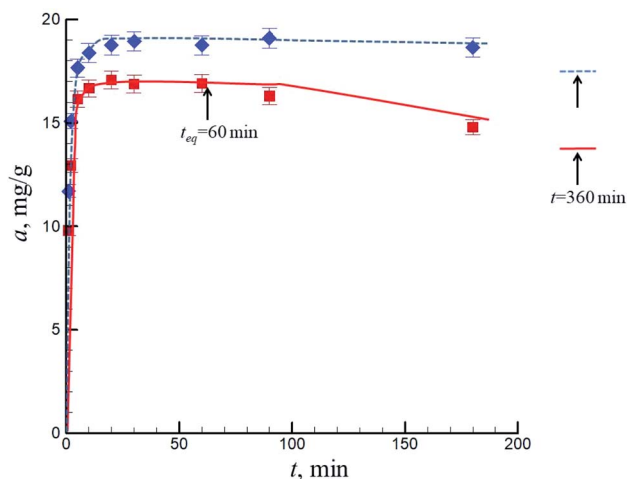


Fig. 6 Time dependencies of Ni(II) adsorption by pristine (squares) and oxidized (diamonds) N-doped CNTs at pH 5.5. The initial concentration of  $\text{NiCl}_2$  in the system was  $50 \text{ mg dm}^{-3}$ .

due to the dissociation of oxidized negative species of various natures on the MWCNTs surface. An increase in the number of oxidized specimen and a decrease in the number of low oxidized groups formed on the surface overcompensate the contribution of the positive surface charge.

### Kinetics of adsorption

Fig. 6 demonstrates the time dependencies of adsorption of Ni(II) ions by pristine and oxidized N-CNT at pH 5.5. The kinetics of adsorption of heavy-metal ions by carbon-containing sorbents is a rather complex process. Most works consider a two-step adsorption kinetics, *i.e.*, an initial rapid uptake and a much slower second stage of adsorption, which may last for several days and even. Some authors reported an optimal contact duration of several minutes,<sup>20</sup> while others believe that the optimal time required to establish equilibrium is equal to several hundred hours.<sup>21,22</sup> Generally, most authors suppose the optimal contact time to be 1–5 h.

Three regions can be distinguished on the kinetic dependencies of adsorption in our experiments. At N-CNT-solution contact duration  $t \leq 10 \text{ min}$  (region I), the specific adsorption drastically increases with time; in a contact-time range of 10–60/100 min (II), the adsorption equilibrium is established; at  $t > 60/100 \text{ min}$ , Ni(II) ions are in a small amount (up to 10%) desorbed from the CNTs surface (region III). A further increase in the contact time up to 5 days gave an insufficient change (2–3%) in the adsorbed amount. Similar results were obtained while adsorbing Cr(III) ions on the CNTs surface.<sup>4</sup> Contact time  $t_{\text{eq}} = 60 \text{ min}$  was chosen to measure the equilibrium adsorption isotherms. The data in Fig. 6 show that this time is enough to establish the adsorption equilibrium.

### Effect of pH on Ni(II) adsorption

Inspecting the effect of pH on the adsorption of Ni(II) ions by carbon nanotubes quite different effects should be considered:

(i) Ni(II) ions in aqueous solutions are hydrated by six water molecules, they possess moderate resistance to hydrolysis and predominantly exist in the form of species with charge 2+ in dilute solutions. Hydrolysis products of  $\text{Ni}(\text{OH})^+$  were found at concentration of salts higher than  $5 \times 10^{-2} \text{ M}$  of Ni(II).<sup>23</sup> The equilibrium constant of formation of  $\text{Ni}(\text{OH})^+$  was determined as  $-19.8$ .<sup>24</sup> Obviously, hydrolysis of nickel salt with a release of  $\text{H}^+$  ions results in a change of the surface charge of N-CNTs (see above) and possibly the adsorption of Ni(II) ions.

(ii) Increasing the system pH gives a rise to the negative surface charge density of N-CNTs and to the adsorption of positively charged nickel ions *via* electrostatic mechanism.

(iii) At pH 7.8–8.0 the process of precipitation of  $\text{Ni}(\text{OH})_2$  starts<sup>24</sup> which leads to pseudo-adsorption of the metal ion on the nanotubes surface.

Detailed information about the changes of the pH in N-CNT suspensions containing permanent amounts of nanotubes and  $\text{NiCl}_2$  at various initial/adjusted pH, can be extracted from the data presented in Table 1. Different behaviour of suspensions having various adjusted pH values should be noticed. Addition of N-CNTs to Ni(II) solutions in acidic media (approximately pH

Table 1 Changes of the equilibrium pH (pH eq.) of 0.1% N-CNT suspensions containing 29–31 mg Ni(II) ions per g carbon nanotubes at various initial/adjusted pH (pH adjust.) of the system

Pristine N-CNTs			Oxidized N-CNTs		
pH adjust.	pH eq.	Adsorption, $\text{mg g}^{-1}$	pH adjust.	pH eq.	Adsorption, $\text{mg g}^{-1}$
2.00	2.04	2.76	2.01	2.03	4.48
2.83	3.48	7.14	2.84	3.18	9.5
4.20	5.43	14.5	4.11	4.93	18.0
5.23	6.18	17.8	5.36	5.23	18.1
6.58	6.50	17.7	6.38	5.26	18.4
7.07	6.82	17.7	7.10	5.26	20.1
8.32	7.04	18.3	8.25	5.60	20.2
8.77	7.64	20.2	8.77	6.58	27.7
10.2	8.84	28.1	9.83	7.21	27.9
11.3	9.70	28.8	11.2	7.74	28.2
11.9	11.4	29.6	11.9	11.0	29.5



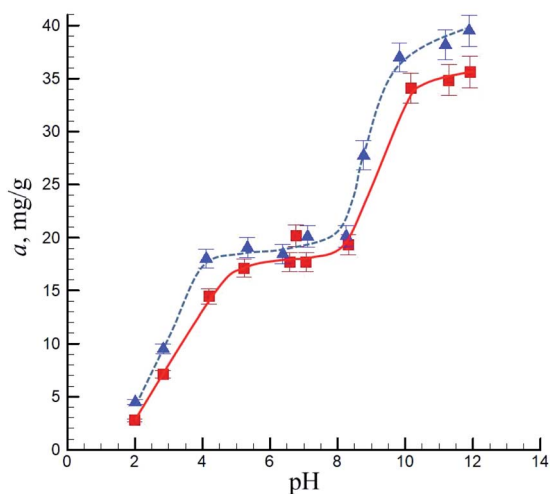


Fig. 7 Adsorbed amount of nickel ions from  $\text{NiCl}_2$  solution by pristine (squares) and oxidized (triangles) N-CNTs as a function of the adjusted pH.

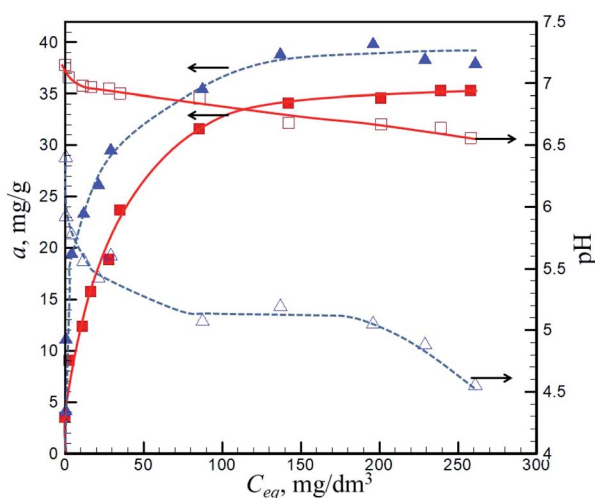


Fig. 8 Adsorption isotherms of  $\text{Ni}(\text{II})$  ions from  $\text{NiCl}_2$  solution by pristine (lower curve) and oxidized (upper curve) N-doped CNTs at "natural" pH of the suspension (pH 5.0–6.0). The change in the equilibrium pH of a 0.1% suspension as a result of adsorption.

2–5 for pristine and pH 2–4 for oxidized samples) results in a measurable increase of the suspension pH. We attribute this rise in pH to transfer of  $\text{H}^+$  ions from the solution to pyridine N-atoms on the N-CNT surface. *i.e.* we can hardly imagine the substitution of surface hydrogen ions by adsorbing nickel ions in the presence of excess  $\text{H}^+$  ions (low pH) in the system. At higher pH values this effect is overcompensated by the ion-exchange of  $\text{Ni}(\text{II})$  with surface  $\text{H}^+$  ions which gives a moderate

drop in pH for pristine N-CNTs and a much bigger decrease of pH (up to 2.5–2.6 pH unit) for the oxidized samples.

The dependencies of  $\text{Ni}(\text{II})$  adsorption on the adjusted pH values by N-doped carbon nanotubes are shown on Fig. 7. Three regions on these plots can be distinguished: in acidic media (from pH 2.0 to pH 5.0 for pristine sample and to pH 4.0 for the oxidized sample) a marked increase in adsorption with an increase in pH was observed; then in the interval of pH 4.0 or 5.0 to pH 8.0 a roughly constant value of adsorption was measured. After that a sharp elevation in the  $\text{Ni}(\text{II})$  adsorption took place due to precipitation of nickel hydroxide on the surface. The changes of the equilibrium pH of N-CNT suspensions as a result of  $\text{Ni}(\text{II})$  adsorption are discussed below.

Our selective tests testify that up to 95–96% of adsorbed  $\text{Ni}(\text{II})$  ions can be removed from the N-CNTs and oxidized N-CNTs surface by elution using 0.01 M HCl, in line with the results obtained by the authors<sup>9,11</sup> for regular (without N-doping) multi-walled carbon nanotubes.

### Adsorption isotherms

Fig. 8 demonstrates the adsorption isotherms of  $\text{Ni}(\text{II})$  ions onto pristine and oxidized N-doped carbon nanotubes. Also the measured changes in the equilibrium pH in a 0.1% suspension as a result of adsorption are shown. The following features should be stressed: (i) the shape of adsorption isotherms is similar: a stepwise rise in adsorption with increasing the equilibrium concentration of the nickel ions, with a tendency to reach a plateau value of the adsorbed amount; (ii) the maximum adsorbed amount slightly increases while moving from pristine ( $35 \text{ mg g}^{-1}$ ) to oxidized ( $40 \text{ mg g}^{-1}$ ) samples; (iii) adsorption of  $\text{Ni}(\text{II})$  gives a non-sufficient lowering the solution pH for pristine N-CNTs (about 0.7 pH unit, from pH 7.2 to pH 6.5) and a marked lowering for oxidized sample (from pH 6.5 to pH 4.5) as a result of ion exchange of surface  $\text{H}^+$  ions for adsorbing nickel ions.

The shape of adsorption isotherms resembles a Langmuir-type isotherm with formation of a monolayer of  $\text{Ni}(\text{II})$  ions on the surface. We have calculated the parameters of adsorption in the coordinates of the linearized Langmuir equation:

$$C_{\text{eq}}/a = 1/(a_{\infty}K) + C_{\text{eq}}/a_{\infty},$$

where  $C_{\text{eq}}$  is the equilibrium concentration of  $\text{Ni}(\text{II})$  ions in the solution,  $\text{mg dm}^{-3}$ ,  $a$  – the adsorbed amount,  $\text{mg g}^{-1}$ , (or  $\text{mmol g}^{-1}$ ),  $a_{\infty}$  – is the limiting adsorption of  $\text{Ni}(\text{II})$  ions,  $\text{mg g}^{-1}$  (or  $\text{mmol g}^{-1}$ ) and  $K$  is the adsorption equilibrium constant,  $\text{dm}^3 \text{ mol}^{-1}$ . We present the maximal adsorbed amount and  $K$  values also in habitual mol units. As seen from the data presented in Table 2, the values of theoretically possible limiting

Table 2 Calculated parameters of the linearized Langmuir equation

Adsorbent	$1/a_{\infty}$	$K \times 10^3, \text{dm}^3 \text{mol}^{-1}$	$a_{\infty}, \text{mmol g}^{-1}$	$a_{\infty}, \text{mg g}^{-1}$
N-CNTs	1.136	6.84	0.44	25.8
Oxidized N-CNTs	1.006	13.65	0.50	29.2



adsorption are close to each other and to the plateau values shown in Fig. 8. The equilibrium constant  $K$  which is proportional to the adsorbate affinity for an adsorbent, is roughly two times higher for oxidized N-CNTs than the value obtained for the pristine sample.

## Discussion

It is demonstrated that N-doped multi-walled carbon nanotubes can serve for extraction of Ni(II) ions from aqueous solution. The specific adsorption values ( $35\text{--}40\text{ mg g}^{-1}$ ) and degree of extraction ( $30\text{--}95\%$  from  $\text{NiCl}_2$  solutions of concentration  $294\text{--}2.6\text{ mg dm}^{-3}$ ) are comparable with those for non-oxidized and oxidized MWCNT, *i.e.* without incorporated N atoms, described in the literature.<sup>1,3,7–9</sup> The main laws of adsorption observed can be summarized as follows: (i) adsorption of Ni(II) reaches equilibrium value within 20–30 min; (ii) the degree of extraction of nickel ions sharply increases with a decrease in their concentration, (iii) adsorption of Ni(II) by pristine N-CNTs results in a non-sufficient decrease in the pH value of the solution (0.7 pH unit) and in a considerable lowering the pH for oxidized sample (up to 2.5 pH unit); (iv) the adsorption isotherms of Ni(II) can be described by the Langmuir equation; the affinity of Ni(II) ions to the surface, characterized by the  $K$  constant of this equation, showed a twofold increase when moving from as-prepared to oxidized samples; at the same time almost the same maximal values of adsorption were measured, in distinction with adsorption of these ions by MWCNTs,<sup>1,5,6</sup> (v) at pH 8 and higher a sharp increase in adsorption took place.

Obviously, different mechanisms are governing the adsorption of Ni(II) ions by N-doped carbon nanotubes. The release of  $\text{H}^+$  ions from the oxidized N-CNTs testifies the essential role of the ion-exchange in binding the nickel ions for this adsorbent; this mechanism is supported by FTIR data. A sudden rise in adsorption at pH > 8 can be ascribed to the precipitation of  $\text{Ni}(\text{OH})_2$  on the both N-CNT surfaces. To estimate the contribution of the ion-exchange into the adsorption of Ni(II) ions by N-doped carbon nanotubes we have compared the adsorbed amounts with changes of the solution pH, *i.e.* the concentration of substituted  $\text{H}^+$  ions by nickel ions on the surface. For example, adsorption of  $18.3\text{ mg g}^{-1}$  or  $2.8 \times 10^{-4}\text{ mol g}^{-1}$  Ni(II) by pristine N-CNTs resulted in a decrease of solution pH from 8.32 to 7.04 (Table 1). Elementary calculations show that this difference in pH corresponds to appearance of  $1.5 \times 10^{-7}\text{ mol H}^+$  ions in a suspension with 10 mg N-CNTs or  $1.5 \times 10^{-5}\text{ mol H}^+$  ions per g nanotubes which comprises approximately 5% of the adsorbed amount of nickel ions. Quite other situation we have observed for oxidized N-CNTs. At adsorption of  $20.2\text{ mg g}^{-1}$  ( $=3.43 \times 10^{-4}\text{ mol g}^{-1}$ ) Ni(II) the drop in the system pH reached 2.65 pH unit, from 8.25 to 5.60 (Table 1) which corresponds to an increase in the  $\text{H}^+$  concentration from  $5.6 \times 10^{-9}\text{ mol dm}^{-3}$  to  $2.5 \times 10^{-6}\text{ mol dm}^{-3}$ , *i.e.* appearance of approximately  $3.3 \times 10^{-6}\text{ mol H}^+$  in a suspension containing 10 mg N-CNTs or  $3.3 \times 10^{-4}\text{ mol H}^+/\text{g N-CNTs}$ . This amount is practically the same as the adsorbed amount of nickel ions. Similar results were obtained with other Ni(II) concentrations. Note that the plateau adsorbed values by pristine and oxidized

samples do not differ substantially. This means that Ni(II) ions will adsorb by the functionalized surface groups of oxidized N-CNTs preferentially *via* ion-exchange mechanism, and the interaction with incorporated into lattice N atoms plays minor role. In the event of pristine N-CNTs the role of ion-exchange is negligible and the substantial adsorption (surprisingly comparable to that for oxidized samples) is probably due to donor–acceptor interactions between the vacant d-orbitals of the adsorbing Ni(II) ions and free electron pair on the N atoms of the lattice surface. So, if adsorbing nickel (and other transition metal ions) have a choice, they prefer the stronger chemical (ion-exchange) bounding to the N-CNTs surface compared to weaker donor–acceptor interactions. If there are no sites for ion-exchange, these ions can be attached to numerous N-atoms on the surface by weaker bounds. The main paragraph text follows directly on here.

## Conclusions

We describe and discuss in this paper the laws and mechanisms of adsorption of Ni(II) ions by well characterized pristine and oxidized (by treatment with mixture of concentrated nitric and sulphuric acids) N-doped multi-walled carbon nanotubes (N-CNTs).

Three different stages in the kinetics of adsorption of Ni(II) on the N-CNTs surface were discovered, *i.e.* a fast initial increase ( $t = 10\text{--}20\text{ min}$ ) in specific adsorption, a stage of establishment of the equilibrium/plateau value of adsorption ( $t = 10/20\text{--}60/100\text{ min}$ ), and a stage in which a small amount of ions desorbed from the surface ( $t > 60/100\text{ min}$ ). It is shown that adsorption of Ni(II) results in a slight decrease in the suspension pH for pristine N-CNTs (0.5–0.6 pH unit) and a considerable lowering the pH for oxidized sample (up to 2.5 pH unit) which is the evidence of different mechanisms of adsorption. We believe that in the first system the major factor governing the adsorption is the donor–acceptor interaction between free electron pair of the N-atoms incorporated into nanotubes lattice with the vacant d-orbital of the Ni(II) ions, while for the oxidized samples the ion-exchange with a release of  $\text{H}^+$  ions plays decisive role. The adsorption isotherms can be described by the Langmuir equation; and the plateau amounts of adsorption was shown to be almost the same ( $35\text{--}40\text{ mg g}^{-1}$ ) for both as-prepared and oxidized samples. At pH 8 and higher a sharp increase in adsorption was observed which was attributed to nickel hydroxide precipitation.

## Conflicts of interest

There are no conflicts to declare.

## Acknowledgements

This research was supported by the Transcarpathian II Ferenc Rakoczi Hungarian Institute, Beregovo, Ukraine and by the bilateral cooperation project between Hungarian and Ukrainian Academies of Sciences, NMK 2018/37. Also the support by the European Union and the Hungarian State, co-financed by the





European Regional Development Fund in the framework of the GINOP-2.3.4-15-2016-00004 project, aimed to promote the cooperation between the higher education and the industry is acknowledged.

## References

- 1 X. Ren, C. Chen, M. Nagatsu and X. Wang, Carbon nanotubes as adsorbents in environmental pollution management: a review, *Chem. Eng. J.*, 2011, **170**, 395–410.
- 2 Y.-H. Li, S. Wang, J. Wei, X. Zhang, C. Xu, Z. Luan, D. Wu and B. Wei, Lead adsorption on carbon nanotubes, *Chem. Phys. Lett.*, 2002, **357**, 263–266.
- 3 K. Pyrzyńska and M. Bystrzejewski, Comparative study of heavy metal ions sorption onto activated carbon, carbon nanotubes, and carbon-encapsulated magnetic nanoparticles, *Colloids Surf., A*, 2010, **362**, 102–109.
- 4 M. V. Manilo, Z. Z. Choma and S. Barany, Comparative study of Cr(III) adsorption by carbon nanotubes and active carbons, *Colloid J.*, 2017, **79**, 212–218.
- 5 Y. H. Li, S. Wang, Z. Luan, J. Ding, C. Xu and D. Wu, Adsorption of cadmium(II) from aqueous solution by surface oxidized carbon nanotubes, *Carbon*, 2003, **41**, 1057–1062.
- 6 C. Chen and X. Wang, Adsorption of Ni(II) from aqueous solution using oxidized multiwall carbon nanotubes, *Ind. Eng. Chem. Res.*, 2006, **45**, 9144–9149.
- 7 S. Yang, J. Li, D. Shao, J. Hu and X. Wang, Adsorption of Ni(II) on oxidized multi-walled carbon nanotubes: effect of contact time, pH, foreign ions and PAA, *J. Hazard. Mater.*, 2009, **166**, 109–116.
- 8 M. I. Kandah and J. L. Meunier, Removal of nickel ions from water by multi-walled carbon nanotubes, *J. Hazard. Mater.*, 2007, **146**, 283–288.
- 9 C. Lu and C. Liu, Removal of nickel(II) from aqueous solution by carbon nanotubes, *J. Chem. Technol. Biotechnol.*, 2006, **81**, 1932–1940.
- 10 F. Giannakopoulou, C. Haidouti, D. Gasparatos, I. Massas and G. Tsiakatouras, Characterization of multi-walled carbon nanotubes and application for Ni<sup>2+</sup> adsorption from aqueous solutions, *Desalin. Water Treat.*, 2016, **57**, 11623–11630.
- 11 G. P. Rao, C. Lu and F. Su, Sorption of divalent metal ions from aqueous solution by carbon nanotubes: a review, *Sep. Purif. Technol.*, 2007, **58**, 224–231.
- 12 A. Gadhave and J. Waghmare, Removal of heavy metal ions from wastewater by carbon nanotubes (CNTs), *International Journal Of Advanced Chemical Science and Applications*, 2014, **5**(2), 56–67.
- 13 C. Chen, J. Hu, D. Shao, J. Li and X. Wang, Adsorption behavior of multiwall carbon nanotube/iron oxide magnetic composites for Ni(II) and Sr(II), *J. Hazard. Mater.*, 2009, **164**, 923–928.
- 14 Z. Gao, T. J. Bandosz, Z. Zhao, M. Han and J. Qiu, Investigation of factors affecting adsorption of transition metals on oxidized carbon nanotubes, *J. Hazard. Mater.*, 2009, **167**, 357–365.
- 15 L. Vanyorek, G. Muranszky, E. Sikora, X. Pénezeli, Á. Prekoba, A. Kiss, B. Fiser and B. Viskolcz, Synthesis Optimization and Characterization of Nitrogen-Doped Bamboo-Shaped Carbon Nanotubes, *J. Nanosci. Nanotechnol.*, 2019, **19**, 429–435.
- 16 L. Vanyorek, R. Meszaros and S. Barany, Surface and electrosurface characterization of surface-oxidized multi-walled N-doped carbon nanotubes, *Colloids Surf., A*, 2014, **448**, 140–146.
- 17 V. Tucureanu, A. Matei and A. M. Avram, FTIR spectroscopy for carbon family study, *Crit. Rev. Anal. Chem.*, 2016, **46**, 502–520.
- 18 S. Barany, N. Kartel' and R. Meszaros, Electrokinetic potential of multilayer carbon nanotubes in aqueous solutions of electrolytes and surfactants, *Colloid J.*, 2014, **76**, 509–513.
- 19 S. Gómez, N. M. Rendtorff, E. F. Aglietti, Y. Sakka and G. Suárez, Surface modification of multiwall carbon nanotubes by sulfonitric treatment, *Appl. Surf. Sci.*, 2016, **379**, 264–269.
- 20 M. Ajmal, R. A. Rao, R. Ahmad, J. Ahmad and L. A. Rao, Removal and recovery of heavy metals from electroplating wastewater by using Kyanite as an adsorbent, *J. Hazard. Mater.*, 2001, **87**, 127–137.
- 21 K. Csobán, M. Párkányi-Berka, P. Joó and P. Behra, Sorption experiments of Cr(III) onto silica, *Colloids Surf., A*, 1998, **141**, 347–364.
- 22 J. Lakatos, S. D. Brown and C. E. Snape, Coals as sorbents for the removal and reduction of hexavalent chromium from aqueous waste streams, *Fuel*, 2002, **81**, 691–698.
- 23 D. M. Novak-Adamić, B. Čosović, H. Bilinski and M. Branica, Precipitation and hydrolysis of metallic ions-V. Nickel(II) in aqueous solutions, *J. Inorg. Nucl. Chem.*, 1973, **35**, 2371–2382.
- 24 K. A. Burkov, L. S. Lilic and L. G. Sillén, Studies on Hydrolysis of Metal Ions, *Acta Chem. Scand.*, 1965, **19**, 14–30.

